

## Adult cerebellar glioblastoma categorized into a pediatric methylation class with a unique radiological and histological appearance: illustrative case

Takahiro Ono, MD,<sup>1</sup> Felix Hinz,<sup>2</sup> Shogo Tanaka,<sup>1</sup> Masataka Takahashi, MD,<sup>1</sup> Hiroshi Nanjo, MD,<sup>3</sup> Andreas von Deimling, MD,<sup>2</sup> and Hiroaki Shimizu, MD<sup>1</sup>

<sup>1</sup>Department of Neurosurgery, Akita University Graduate School of Medicine, Akita, Japan; <sup>2</sup>Department for Neuropathology and CCU Neuropathology, University of Heidelberg and DKFZ, Heidelberg, Germany; <sup>3</sup>Department of Clinical Pathology, Akita University Hospital, Akita, Japan

**BACKGROUND** Recent studies report that cerebellar glioblastoma (GBM) is categorized into the RTK1 methylation class. GBM pediatric RTK (pedRTK) subtypes are distinct from those of adult GBM. We present a unique adult case of cerebellar GBM classified into the pedRTK subtype.

**OBSERVATIONS** Magnetic resonance imaging revealed a homogeneous enhancing lesion in the right cerebellum in a 56-year-old woman presenting with ataxia and dizziness. Arterial spin labeling and angiographic findings and the intraoperative orange-colored tumor appearance were reminiscent of hemangioblastoma. She showed an atypical presentation in terms of high glucose metabolism. The histological diagnosis was high-grade glioma with differentiation similar to central nervous system neuroblastoma. The methylation class was GBM pedRTK1. Consistent with this classification, immunopositivity was positive for SOX10 and negative for ANKRD55. She underwent craniospinal radiotherapy (23.4 Gy) with a boost to the tumor bed (total 55.8 Gy). Twelve courses of temozolomide therapy were administered. There was no recurrence 18 months after surgery.

**LESSONS** Radiological and intraoperative findings, such as hemangioblastoma and high glucose metabolism, were notable characteristics in the present case. Both glial and neuronal differentiation and SOX10 immunopositivity were presenting pathological features. Similar cerebellar GBMs might form a previously unestablished subtype. Establishing effective molecular diagnoses is important.

<https://thejns.org/doi/abs/10.3171/CASE2260>

**KEYWORDS** methylation profile; glioblastoma; neuroblastoma; hemangioblastoma; SOX10

Adult cerebellar glioblastomas (GBMs) are mostly categorized into proneural type GBMs (RTK1 methylation class) via DNA methylation profile analysis.<sup>1</sup> Studies report that GBM pediatric RTK (pedRTK) subtypes are distinct from adult GBM.<sup>2</sup>

Herein, we present a unique adult case of cerebellar GBM that was categorized into the GBM pedRTK1 methylation class. This case showed not only characteristic radiological and intraoperative findings reminiscent of hemangioblastoma but also uniquely presented with histological differentiation (reminiscent of central nervous system neuroblastoma [CNS NB]). These findings might represent undiscovered clinical and molecular characteristics of a previously uncharacterized adult cerebellar GBM subtype.

### Illustrative Case

A 56-year-old woman presented to her local hospital with dysarthria caused by a right cerebral lacunar infarction and was admitted to this hospital 1 year before the final diagnostic and surgical course reported herein. She had a history of hypertension and hyperlipidemia with no notable family or personal psychosocial history.

Although fluid-attenuated inversion recovery (FLAIR) magnetic resonance imaging (MRI) performed at her local hospital showed a slightly hyperintense lesion in the right cerebellum, she had no cerebellar symptoms. The infarction was treated with antiplatelet therapy, with routine follow-up for the cerebellar lesion.

**ABBREVIATIONS** ASL = arterial spin labeling; CNS NB = central nervous system neuroblastoma; FDG-PET = <sup>18</sup>F-fluorodeoxyglucose–positron emission tomography; FLAIR = fluid-attenuated inversion recovery; GBM = glioblastoma; MRI = magnetic resonance imaging; NGS = next-generation sequencing; pedRTK = pediatric RTK; PCNSL = primary central nervous system lymphoma; SUVmax = maximum standardized uptake value.

**INCLUDE WHEN CITING** Published April 4, 2022; DOI: 10.3171/CASE2260.

**SUBMITTED** February 3, 2022. **ACCEPTED** February 21, 2022.

© 2022 The authors, CC BY-NC-ND 4.0 (<http://creativecommons.org/licenses/by-nc-nd/4.0/>).

One year later, her symptoms of ataxia in the right upper limb and dizziness gradually worsened. MRI revealed not only an enlargement of the FLAIR-hyperintense lesion (Fig. 1A) but also a

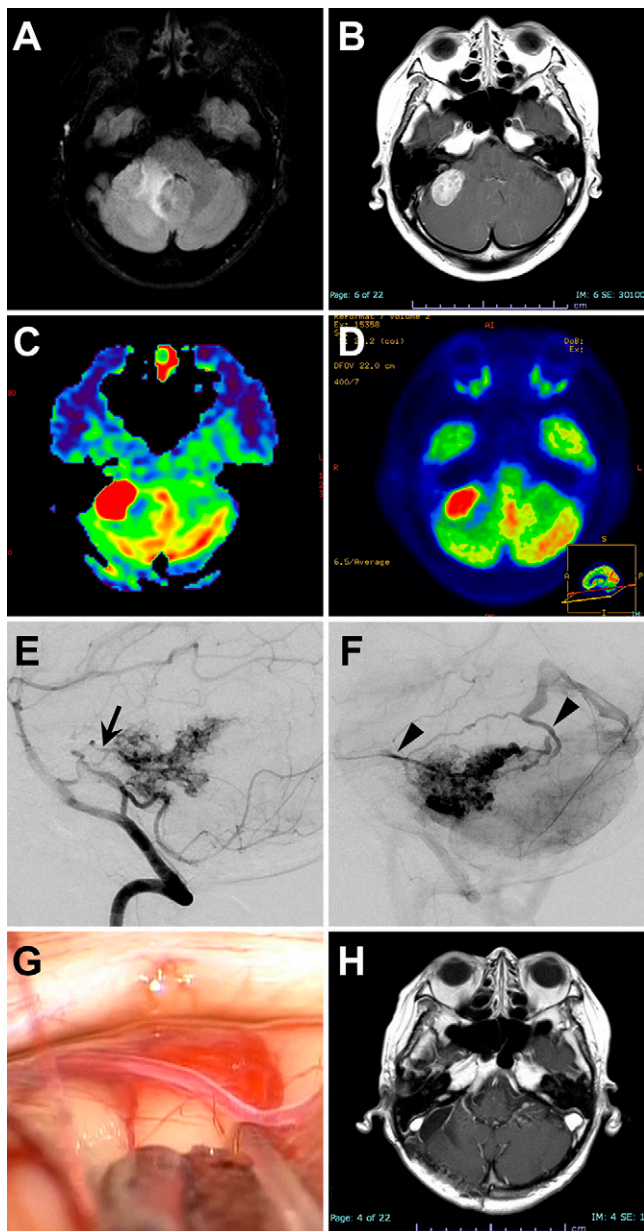


**FIG. 1.** Preoperative FLAIR image showed a hyperintense lesion in the right cerebellum (A), and a postcontrast T1-weighted MRI scan revealed a homogeneously enhanced nodular lesion (B). The nodular lesion showed hyperintensity on ASL (C). FDG-PET (D) revealed high-level tumor glucose metabolism. Preoperative right vertebral artery angiography revealed a marked tumor stain. The main feeding artery was determined to be the right anterior inferior cerebellar artery (arrow, E). Early venous filling of the tentorial and superior petrosal sinus (right and left arrowheads, respectively) were observed in the late arterial phase (F). Intraoperative findings (G) through a right lateral suboccipital approach. The orange-colored tumor beside the feeding artery was exposed on the cerebellar surface. Postcontrast T1-weighted MRI (H) conducted 18 months after surgery showed no recurrence.

new homogeneously enhanced nodular lesion (Fig. 1B). The patient was referred to our department for additional evaluation.

Arterial spin labeling (ASL) showed marked hyperintensity in the nodular lesion (Fig. 1C) and  $^{18}\text{F}$ -fluorodeoxyglucose–positron emission tomography (FDG-PET) revealed high glucose metabolism (maximum standardized uptake value [SUVmax] 20.5; tumor-to-nontumor ratio 1.59; Fig. 1D). There were no abnormalities seen on a whole-body PET scan. Angiography of the right vertebral artery revealed marked tumor staining. A branch of the anterior inferior cerebellar artery was the main feeding source for the tumor (Fig. 1E). Early venous filling to the tentorial and superior petrosal sinus was observed in the late arterial phase (Fig. 1F).

The initial (preliminary) preoperative diagnosis was hemangioblastoma. However, the patient's clinical course (i.e., the enhancing nodule enlarged within 1 year) and the finding of high FDG uptake were inconsistent with the features of a benign tumor. Hence, a malignancy could not be ruled out. We planned to perform surgical resection followed by an applicable aftertreatment based on the resulting histological diagnosis.

The surgery was performed using the right lateral suboccipital approach. An orange-colored tumor located beside the feeding artery was observed after retraction of the right cerebellum (Fig. 1G). The tumor appearance was consistent with hemangioblastoma. However, the boundary with the normal cerebellum was poorly demarcated, and the tumor bled easily (thus denoting an atypical presentation). The tumor was removed en bloc while the feeding branches were cauterized. The resected sample was gelatinous and cell-rich, which differed from the typical macroscopic findings of hemangioblastoma.

### Histopathological and Molecular Findings

Hematoxylin-eosin staining revealed a marked proliferation of relatively monomorphic tumor cells with a high nuclear-to-cytoplasm ratio. In addition to glial differentiation, we found a cellular palisading pattern (Fig. 2A) and a neuropil island (Fig. 2B). Multiple malignant tumors with a small, round, and blue-cell appearance were compatible with a diagnosis of either GBM or CNS NB. Because a rare brain tumor was suspected, the Japan Brain Tumor Reference Center (Maebashi, Japan) was contacted for a central review.

Immunohistochemical staining was positive for nestin (Fig. 2C), CD56 (Fig. 2D), Olig2 (Fig. 2E), ATRX, and H3K27me3, partially positive for synaptophysin (Fig. 2F), glial fibrillary acidic protein (Fig. 2G), and neurofilament, and negative for IDH1 R132H, CD99, chromogranin A, H3.3K27M, and p53. The Ki-67 index was 39.9% (Fig. 2H). Although the expression of glial markers suggested a diagnosis of high-grade glioma, it was difficult to confirm the subclassification.

We then consulted Heidelberg University (Heidelberg, Germany) to obtain molecular analyses using methylation-based classification,<sup>3</sup> a next-generation sequencing (NGS) panel,<sup>4</sup> and additional immunohistochemical staining. In the methylation-based classification, the present tumor was localized into the GBM pedRTK1 cluster (Fig. 3A) and thus differed from previously characterized adult GBMs and CNS NBs.

The copy number variation profile revealed a *CDKN2A/B* homozygous deletion (Fig. 3B), and NGS demonstrated mutations in *SMO*, *FGFR1*, and *NF1*. The present case was positive for SOX10 but negative for ANKRD55 upon additional immunohistochemical staining (Fig. 4A and B). These findings were consistent with a diagnosis of GBM pedRTK1.<sup>5–8</sup> However, the profiled case presented with an adult cerebellar tumor. The final integrated diagnosis was cerebellar GBM with no established reference class.

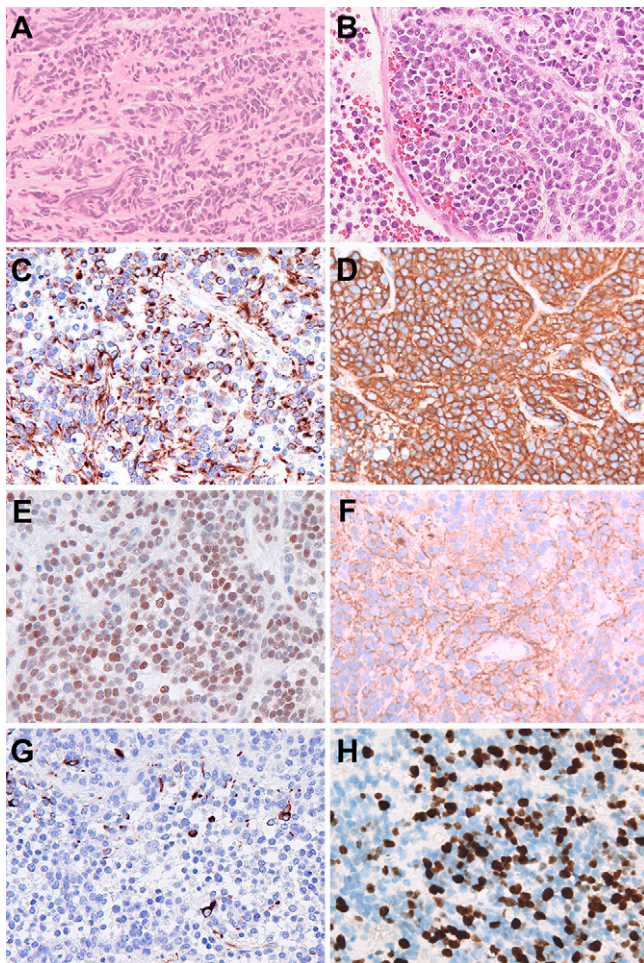


**FIG. 2.** Representative pathological findings. Hematoxylin and eosin staining revealed a cellular palisading pattern (A) and a neuropil island (B). Immunohistochemical staining findings. The tumor cells were positive for nestin (C), CD56 (D), and Olig2 (E) and were partially positive for synaptophysin (F) and glial fibrillary acidic protein (G). The Ki-67 index was 39.9% (H). Original magnification  $\times 200$ .

### Postoperative Course

Postoperative MRI demonstrated that the solid enhancing lesion was completely removed. Although the patient continued to present with ataxia in the right upper and lower limbs, these lingering symptoms improved 2 weeks after surgery. During the diagnostic consultation, she underwent craniospinal radiotherapy (23.4 Gy) with a three-dimensional conformal boost to the tumor bed (total dose 55.8 Gy) according to the standard treatment protocol frequently employed for embryonal tumors.<sup>9,10</sup> After radiotherapy, she was discharged without any neurological deficits. A total of 12 courses of temozolomide maintenance therapy (4-week cycles) were administered based on her integrated diagnosis. Eighteen months after surgery, MRI showed no evidence of tumor recurrence (Fig. 1H).

### Discussion

Herein, we report a case of adult cerebellar GBM with unique radiological, pathological, and molecular characteristics. Representative cerebellar tumors in adults include GBM, hemangioblastoma,

and primary central nervous system lymphoma (PCNSL).<sup>11,12</sup> The radiological features of these tumors differ substantially, and preoperative differentiation is thus generally possible.

The present case demonstrated a solid and homogeneous enhancing lesion upon MRI as well as marked tumor staining upon angiography. These findings were consistent with a diagnosis of hemangioblastoma. The intraoperative orange-colored tumor appearance was likewise reminiscent of hemangioblastoma. However, a previous study reported lower FDG uptake levels in hemangioblastoma ( $SUV_{max} 4.3 \pm 0.65$ ; mean  $\pm$  standard deviation) as compared with malignant cerebellar tumors, including GBM, PCNSL, and metastatic brain tumors ( $SUV_{max} 13.4 \pm 3.5$ ).<sup>13</sup> The FDG uptake in the present case ( $SUV_{max} 20.5$ ) was extremely high, thus indicating the presence of malignancy.

Based on the findings of contrast-enhanced MRI and FDG-PET, PCNSL was included within the differential diagnosis. However, PCNSL is traditionally reported to be avascular on angiography.<sup>14</sup> Moreover, our previously published data have demonstrated that ASL is not hyperintense in PCNSL.<sup>15</sup> The angiography and ASL findings in the present case differed from those of PCNSL, thus supporting our determination of surgical resection.

The findings of light microscopy examination in the present case demonstrated both neuronal and glial differentiation. Moreover, the expression of glial markers and the methylation-based classification supported a diagnosis of GBM RTK1 and was suggestive of the GBM pediatric subtype. The immunohistochemical findings in the present case, which was positive for SOX10 and negative for ANKRD55, were consistent with this diagnosis.<sup>6</sup>

The SOX10 gene has been reported to be a master regulator based on the epigenomic profiling of GBM RTK1 and has been suggested to have a favorable prognosis.<sup>16</sup> This could explain the favorable clinical course seen in the present case. In addition, SOX10 encodes a transcription factor mediating the differentiation of neural crest cells,<sup>17–19</sup> and its expression is found not only in neuroblastomas but also in diffuse gliomas.<sup>19,20</sup> In fact, a previously reported case of CNS NB presenting with both neuronal and glial differentiation was recently reported.<sup>21</sup> This case was classified as CNS NB with FOXR2 activation, and the differentiating characteristic was the high-level expression of SOX10.<sup>6,22</sup> High SOX10 expression may have mediated the confusing histology within the present case.

### Observations

Integrating the comprehensive information presented herein, the ultimate diagnosis of the present case was consistent with GBM pedRTK1. However, in this regard, we forewarn that “pedRTK1” is the name of a methylation-based class that is relevant to pediatric brain tumors. Whether this methylation class is applicable to adult cases in general or to adult cerebellar GBMs specifically has not been investigated to date. To our knowledge, the present case is the first case of adult cerebellar GBM that has been classified into the pedRTK1 methylation class through detailed molecular analyses. The clinical and molecular characteristics of this methylation class need to be elucidated more comprehensively through an additional accumulation of cases.

### Lessons

Herein, we present a unique adult case of cerebellar GBM that was classified into the GBM pedRTK1 methylation class. Radiological and intraoperative findings, including findings reminiscent of hemangioblastoma and high FDG uptake levels, were notable



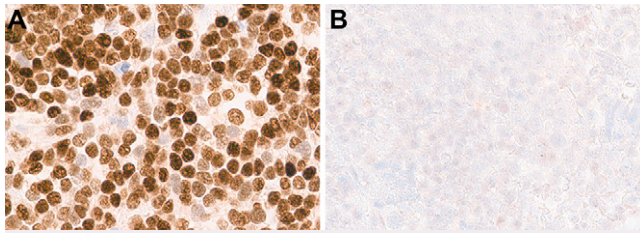


**FIG. 4.** The findings of additional immunohistochemical staining. The tumor cells were mostly positive for SOX10 (A) and negative for ANKRD55 (B). Original magnification  $\times 400$ .

## Acknowledgments

Molecular diagnoses in this study were performed using a grant from the Japan Society for the Promotion of Science (KAKENHI, grant number JP19K16823, awarded to T.O.).

## References

- Nomura M, Mukasa A, Nagae G, et al. Distinct molecular profile of diffuse cerebellar gliomas. *Acta Neuropathol.* 2017;134(6):941–956.
- Korshunov A, Schrimpf D, Ryzhova M, et al. H3-/IDH-wild type pediatric glioblastoma is comprised of molecularly and prognostically distinct subtypes with associated oncogenic drivers. *Acta Neuropathol.* 2017;134(3):507–516.
- Capper D, Jones DTW, Sill M, et al. DNA methylation-based classification of central nervous system tumours. *Nature.* 2018;555(7697):469–474.
- Sahm F, Schrimpf D, Jones DT, et al. Next-generation sequencing in routine brain tumor diagnostics enables an integrated diagnosis and identifies actionable targets. *Acta Neuropathol.* 2016;131(6):903–910.
- Brennan CW, Verhaak RG, McKenna A, et al. The somatic genomic landscape of glioblastoma. *Cell.* 2013;155(2):462–477.
- Korshunov A, Okonechnikov K, Schmitt-Hoffner F, et al. Molecular analysis of pediatric CNS-PNET revealed nosologic heterogeneity and potent diagnostic markers for CNS neuroblastoma with FOXR2-activation. *Acta Neuropathol Commun.* 2021;9(1):20.
- Sturm D, Witt H, Hovestadt V, et al. Hotspot mutations in H3F3A and IDH1 define distinct epigenetic and biological subgroups of glioblastoma. *Cancer Cell.* 2012;22(4):425–437.
- Suzuki H, Aoki K, Chiba K, et al. Mutational landscape and clonal architecture in grade II and III gliomas. *Nat Genet.* 2015;47(5):458–468.
- Gajjar A, Chintagumpala M, Ashley D, et al. Risk-adapted craniospinal radiotherapy followed by high-dose chemotherapy and stem-cell rescue in children with newly diagnosed medulloblastoma (St Jude Medulloblastoma-96): long-term results from a prospective, multi-centre trial. *Lancet Oncol.* 2006;7(10):813–820.
- Packer RJ, Gajjar A, Vezina G, et al. Phase III study of craniospinal radiation therapy followed by adjuvant chemotherapy for newly diagnosed average-risk medulloblastoma. *J Clin Oncol.* 2006;24(25):4202–4208.
- Louis DOH, Wiestler OD, Cavenee WK, eds. *World Health Organization classification of tumours.* 5th ed. Lyon, France: IARC Press; 2021.
- Anonymous. Brain Tumor Registry of Japan (2005-2008). *Neurol Med Chir (Tokyo).* 2017;57(Suppl 1):9–102.
- Takahashi Y, Nishio A, Yamamoto D, Kamada H, Hashimoto N. Usefulness of  $^{18}\text{F}$ -fluorodeoxyglucose-positron emission tomography in comparison with methionine-positron emission tomography in differentiating solid hemangioblastoma from adult cerebellar tumors. *World Neurosurg.* 2018;110:e648–e652.
- Helle TL, Britt RH, Colby TV. Primary lymphoma of the central nervous system. Clinicopathological study of experience at Stanford. *J Neurosurg.* 1984;60(1):94–103.
- Hatakeyama J, Ono T, Takahashi M, Oda M, Shimizu H. Differentiating between primary central nervous system lymphoma and glioblastoma: the diagnostic value of combining  $^{18}\text{F}$ -fluorodeoxyglucose positron emission tomography with arterial spin labeling. *Neurol Med Chir (Tokyo).* 2021;61(6):367–375.
- Wu Y, Fletcher M, Gu Z, et al. Glioblastoma epigenome profiling identifies SOX10 as a master regulator of molecular tumour subtype. *Nat Commun.* 2020;11(1):6434.
- Mollaaghbabab R, Pavan WJ. The importance of having your SOX on: role of SOX10 in the development of neural crest-derived melanocytes and glia. *Oncogene.* 2003;22(20):3024–3034.
- Kelsh RN. Sorting out Sox10 functions in neural crest development. *BioEssays.* 2006;28(8):788–798.
- Miettinen M, McCue PA, Sarlomo-Rikala M, et al. Sox10—a marker for not only schwannian and melanocytic neoplasms but also myoepithelial cell tumors of soft tissue: a systematic analysis of 5134 tumors. *Am J Surg Pathol.* 2015;39(6):826–835.
- Kordes U, Hagemel C. Expression of SOX9 and SOX10 in central neuroepithelial tumor. *J Neurooncol.* 2006;80(2):151–155.
- Furuta T, Moritsubo M, Muta H, et al. Central nervous system neuroblastoma with FOXR2 activation presenting both neuronal and glial differentiation: a case report. *Brain Tumor Pathol.* 2020;37(3):100–104.
- Sturm D, Orr BA, Toprak UH, et al. New Brain Tumor Entities Emerge from Molecular Classification of CNS-PNETs. *Cell.* 2016;164(5):1060–1072.

## Disclosures

Dr. von Deimling reported a patent issued for a DNA methylation-based method for classifying tumor species (EP16710700). No other disclosures were reported.

## Author Contributions

Conception and design: Ono, Tanaka, Takahashi. Acquisition of data: Ono, Hinz, Takahashi, von Deimling. Analysis and interpretation of data: Ono, Hinz, Nanjo, von Deimling. Drafting the article: Ono, Shimizu. Critically revising the article: Ono, von Deimling, Shimizu. Reviewed submitted version of manuscript: Ono, Takahashi, Nanjo, von Deimling, Shimizu. Approved the final version of the manuscript on behalf of all authors: Ono. Administrative/technical/material support: Nanjo, von Deimling.

## Correspondence

Takahiro Ono: Akita University Graduate School of Medicine, Akita, Japan. t.ono@med.akita-u.ac.jp.